Natural Convection in a Vertical Annulus with Constant Heat Flux on the Inner Wall

الحمل الطبيعي فى وسط حلقي رأسي معرض لفيض حراري ثابت عند السطح الداخلي

M.S. El-Kady, and F. F. Araid

Mechanical Power Engineering Department
Mansoura University, Egypt

خلاصـــــة:

يتناول البحث دراسة نظرية وعملية لانتقال الحرارة بالحمل الطبيعى للهواء خلال وسط حلقى رأسى معرض لفيض حرارى ثابت عند الجدار الداخلي وسطح خارجى عند درجة حرارة ثابتة. والدراسة النظرية تهدف الى دراسة تأثير نسبة الأقطار للوسط الحلقى على شكل سريان المائع وانتقال الحرارة. وتكون النموذج من معادلات كمية الحركة والطاقة، واستخدمت طريقة الفروق المحددة للحل العددى. أجريت الدراسة على وسط حلقى ذو نسبة باعية (الارتفاع الى سمك الوسط الحلقى) A=2 وعدد رايلى يصل الى 10^7 ونسبة أقطار للوسط الحلقى $1.2 \le k \le 10$. أظهرت النتائج تأثيرا ملحوظا لنسبة الأقطار على خواص انتقال الحرارة وسريان المائع وعلى العوامل المؤثرة عليهما كسرعة المائع وتوزيع درجات الحرارة داخل الوسط الحلقى.
ولاثبات صحة النموذج النظرى أجريت دراسة عملية لنسبة باعية A=2 , $k = 41$، وقد قورنت النتائج العملية على شكل عدد نوسيلت- عدد رايلى مع النتائج العددية المناظرة، كما تم مقارنة النتائج العملية والنظرية بالنتائج المتاحة فى هذا المجال [١ و ٦] والتى اظهرت توافقا كبيرا بينهما.

Abstract:

Numerical and experimental study is carried out for the steady laminar natural convection of air in a vertical annulus with constant heat flux heated inner wall and an isothermally cooled outer wall. The primary objective for the numerical study is to show the effect of the radius ratio of the vertical annulus on the fluid flow structure and heat transfer. The momentum and energy equations are used for the numerical model and are solved numerically by the finite difference technique. Results are generated for flow in an annulus with aspect ratio A=2, Rayleigh number $10^3 \le Ra \le 10^6$ and radius ratio $1.2 \le k \le 10$. The results clearly indicate that the radius ratio has a significant influence on the heat transfer characteristics and fluid flow structure and the factors affecting it such as the velocity and temperature distribution for the flow inside the annulus. An experimental test was made for the case of A = 2, $k = 41$ and the measured Nusselt number was compared with the computed one to show the validity of the numerical simulation. Another comparison was done with the results of Sheriff [1] and Keyhani et al. [6].

Accepted May 21, 1998

1. Introduction

Natural convection heat transfer in enclosures commonly occurs in nature, and in engineering and technological applications. This Phenomenon plays an important role in such diverse applications including heat exchangers, food industry, biomedical applications and heat transfer from a nuclear fuel rod bundle in nuclear reactors and the interior of its canister in either storage or disposal.

In these cases, the fluid is driven by density variations in a body force field, and the flow pattern depends critically on the applied heating conditions at the boundaries. These kind of flow systems are governed by the Navier-Stokes equations, but, due to the complexity of the equations and the coupling of the dependent variables, general analytical solutions are still not possible. Most previous research efforts have been based on experimental work and, recently, on numerical approaches.

Sheriff [1] conducted experiments with CO_2-filled vertical annuli of radius ratio k=1.03, 1.11 and 1.23 for the height to gab width ratio A= 38,76 and 228. The inner cylinder in his experiments was heated by applying a uniform heat flux and the outer cylinder was halted at constant temperature. The obtained heat transfer correlation for boundary layer regime:

$$\bar{Nu} = 0.3325\ Ra^{0.231}\ A^{-0.25} \qquad (1)$$

which did not show any radius ratio dependence owing to the considered small range of radius ratio (close to unity). Utilizing a double boundary layer model, Nagendra et al. [2] developed an approximate analysis for the isothermally heated vertical annuli. Their analysis suffers from a large discrepancy in the energy balance due to the logarithmic nature of conduction temperature profile. The first extensive study of free convection in isothermally heated vertical annuli was reported by de Vahl Davis and Thomas [3], which was further extended by Thomas and de Vahl Davis [4]. They solved the governing equation for $Ra \le 2\times10^5$, $1 \le A \le 20$ and the majority of the results were obtained for Pr =1 and $1 \le k \le 4$. They reported the Nusselt number dependence on the radius and aspect ratios for the boundary layer regime as $k^{0.442}$ and $A^{-0.238}$ respectively. Another attempt to solve the problem by using a finite difference method was made by Schwab and Dewitt [5]. The heat transfer results obtained by them are quite limited (only 24 combinations of Ra, Pr, and A with k=2). Keyhani et al. [6] conducted experiments with air and helium as test fluids for the case when a constant heat flux is applied on the inner wall of the annulus for k=4.33 and A=27.6 and a wide range of Rayleigh number. Bhushan et al. [7] extended this work for two other combinations of aspect and radius ratios, A=52.52, k=2.77 and A=38.38 and k=8.25 and presented heat transfer correlations for various regimes. Prasad and Kulacki [8] performed experiments with a liquid-filled annulus for k=5.338, aspect ratio A=0.5, 1, and 1.5. Water and ethylene glycol were used as the working fluids enclosed in a vertical annulus with isothermal boundary conditions on both inner and outer walls. For steady natural convection of water near 4°C, i.e. the existence of an anomalous density-temperature relationship fluids, Lin and Nansteel [9] studied numerically the flow in a vertical annulus with isothermal inner and outer boundaries for $10^3 \le Ra \le 10^5$, $1 \le A \le 20$ and varying degrees of curvature. Their results show that the annulus curvature have a strong effect on the flow structure and heat transfer in the annulus.

While Ho and Lin [10] discussed how the mixed boundary conditions influence the heat and fluid flow structures of natural convection of cold water in a vertical annulus. Their results indicate that the mixed boundary conditions can have a significant influence on the geometric dependence of heat transfer characteristics and fluid flow structures in comparison with those reported for isothermal boundary conditions.

From this literature review, it is clear that the curvature (radius ratio) effects on the fluid flow structure and heat transfer in a vertical annulus are not well understood, especially for the buoyancy induced flow for both the constant heat flux and the isothermal boundary conditions at the inner surface of the annulus. In the present study, the governing equations for the problem under consideration are solved numerically using the finite difference method. The primary objective is to examine the effect of the radius ratio of the vertical annulus on the fluid flow structure and heat transfer for the natural convection of the buoyancy induced flow under the influence of the constant heat flux condition at the inner surface of the annulus. An experimental test was made for the case of air flow with Pr = 0.7, A= 2, k = 41 for $10^3 \le Ra \le 10^6$ and the measured Nusselt number was compared with the calculated one to show the validity of the numerical simulation. Also a comparison was done with the results of Sheriff [1] and Keyhani et al. [6].

2. Mathematical Formulation and Method of Solution

Consider the air filled annular region with height H, and inner and outer radii r_i and r_o, respectively (gab width $D = r_o - r_i$) shown in Fig. 1. The outer wall is at constant temperature T_o and the inner wall is exposed to constant heat flux q, while the horizontal surfaces are insulated. Assuming that the fluid properties are constant except for density in the buoyancy term of the vertical momentum balance, the governing equations for momentum with the Bousinisq approximation and energy in the annulus expressed in steady dimensional form are:

$$u\,\partial u/\partial r + v\,\partial u/\partial z = -1/\rho.[\partial P/\partial r] + \upsilon.[\partial^2 u/\partial r^2 + 1/r.(\partial u/\partial r) + \partial^2 u/\partial z^2 - u/r^2] \quad (2)$$

$$u\,\partial v/\partial r + v\,\partial v/\partial z = -1/\rho.[\partial P/\partial z] + \upsilon.[\partial^2 v/\partial r^2 + 1/r.(\partial v/\partial r) + \partial^2 v/\partial z^2] + g\beta(T-T_o) \quad (3)$$

$$u\,\partial T/\partial r + v\,\partial T/\partial z = \alpha.[\partial^2 T/\partial r^2 + 1/r.(\partial T/\partial r) + \partial^2 T/\partial z^2] \quad (4)$$

and the conditions on the boundaries are $u = v = 0$, $q(r_i,z)$ = constant , $T(r_o,z) = T_o$, and $\partial T(r,0)/\partial z = \partial T(r,H)/\partial z = 0$

where υ, v, P, ρ, υ, and α are the velocity in the radial and axial directions r and z, the pressure, the fluid density, the fluid dynamic viscosity and the thermal diffusivity respectively.

The pressure P can be eliminated from equations (2) and (3) by differentiating Eq. (2) with respect to r and Eq. (3) with respect to z and subtracting them. From the definitions $\zeta = \partial v/\partial r - \partial u/\partial z$, $u = 1/r.(\partial\psi/\partial z)$ and $v = -1/r.(\partial\psi/\partial r)$ and using the nondimensional variables: $R = r/D$, $Z = z/D$, $U = u.D/\alpha$, $V = v.D/\alpha$, $\omega = \zeta.D^2/\alpha$, $\Psi = \psi/(\alpha D)$, and $\theta = (T - T_o)/(q.D/k)$ the dimensionless form for the governing

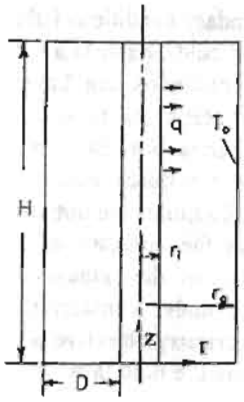

Fig. 1 Physical model, coordinate system and boundaries

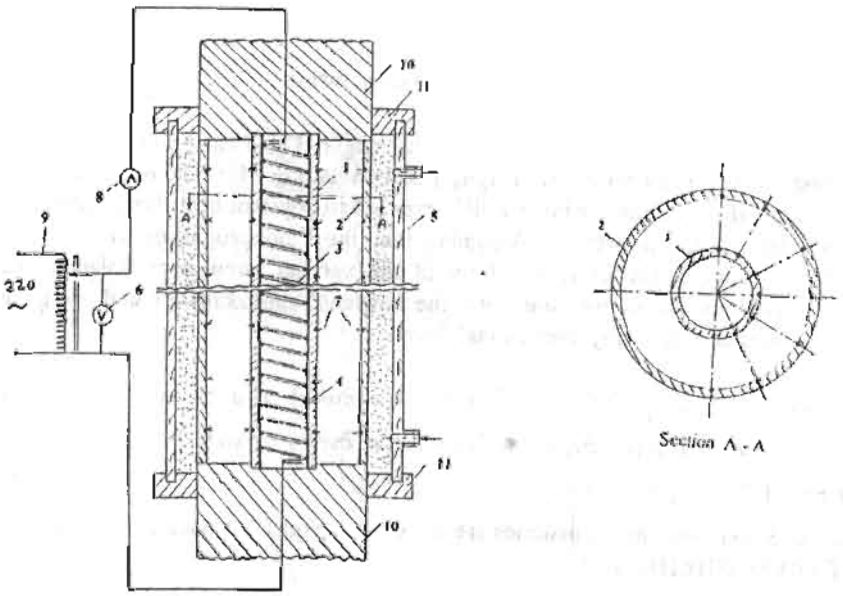

Fig. 2 Schematic diagram of the experimental apparatus

(1) brass inner tube, (2) outer brass tube, (3) nickel-chrome electric heater, (4) pyrex tube, (5) water cooling jacket, (6) voltmeter, (7) copper-constantan thermocouple, (8) ammeter, (9) auto-transformer, (10) Teflon connections, and (11) cooling jacket cover.

equations (2-4) for steady axisymmetric laminar natural convection in a vertical annulus can be written in terms of stream function, vorticity, radial and axial velocities and temperature as follows:

$$U.\partial\omega/\partial R+V.\partial\omega/\partial Z-U\omega/R= Ra.Pr.[\partial\theta/\partial R]+Pr.[\partial^2\omega/\partial R^2+1/R(\partial\omega/\partial R)+\partial^2\omega/\partial Z^2-\omega/R^2] \quad (5)$$

$$-\omega R = \partial^2\Psi/\partial R^2-1/R(\partial\Psi/\partial R)+\partial^2\Psi/\partial Z^2 \quad (6)$$

$$U.\partial\theta/\partial R+V.\partial\theta/\partial Z-U\theta/R= \partial^2\theta/\partial R^2+1/R(\partial\theta/\partial R)+\partial^2\theta/\partial Z^2 \quad (7)$$

$$U=1/R.(\partial\Psi/\partial Z) \text{ and } V=-1/R.(\partial\Psi/\partial R) \quad (8)$$

and the dimensionless boundary conditions for the present system are

$$\partial\Psi/\partial R = \partial\Psi/\partial Z = \Psi = 0, \text{ on all boundaries} \quad (9a)$$

$$\partial\theta/\partial R = -1 \quad \text{at } R= 1/(k-1) \quad (9b)$$

$$\theta = 0 \quad \text{at } R= k/(k-1) \quad (9c)$$

$$\partial\theta/\partial Z = 0 \quad \text{at } Z=0 \text{ or } A \quad (9d)$$

where k is the thermal conductivity, k is the radius ratio, Pr is the Prandtle number and the Rayleigh number $Ra = g\,\beta\,D^4\,q\,/(k\alpha\upsilon)$

The dimensionless governing equations (5-8) and the associated boundary conditions given by equation (9) were solved by a finite difference method. Both the first and second order derivatives were discretized using central difference formulas [11] except the convection terms which were discretized by using the upwind scheme. The difference algebraic equations are solved using the Gauss-elimination method [11]. An iterative solution procedure was employed here to obtain the steady state solution of the problem considered. The convergence criteria used for all field variables $\xi(=\omega, \Psi, \theta)$ for every point are as follows:

$$|\xi^{n+1}-\xi^{n}|_{max} \;/\; |\xi^{n+1}|_{max} \le 10^{-5}$$

where n is the index representing the iteration number.

3. The Experimental Work:

To validate the program developed for this study an experimental study for the air flow in an annulus is carried out. A schematic diagram of the test rig is shown in Fig. 2. The test section is made of a brass inner tube (1) of 21 mm outside diameter, and 492 mm long. The tube is supported concentrically in an outer brass tube (2) of 45 mm inside diameter and 492 mm long. The inner tube is machined to have enough space where an electrical resistance nickel-chrome heater (3) is fitted into a pyrex tube (4) and inserted through it to give constant heat flux along the length of the inner tube. A water cooling jacket (5) is made around the outer surface of the outer tube to maintain a constant wall temperature. The voltage drop over the electrical resistance is measured by a voltmeter (6), which in turn provides the heat flow rate from the inner tube to the convection medium. The temperature of the inner tube surface is measured

by 15 copper-constantan thermocouples (7) equally spaced distributed along the tube length and 30° apart along one half of the tube section as shown in Fig. 2. The surface temperature of the outer tube is measured by 15 copper-constantan thermocouples distributed in the same way as in the inner one. To reach the steady state, every test was run for nearly three hours. This was verified by recording the surface temperature and noticing its variations.

4. Results and Discussion

The range of parameters considered in the present study is Pr =0.7, A=2, $10^3 \leq Ra \leq 10^7$, and radius ratio $1.1 \leq k \leq 10$. The results are presented in the form of streamline and isotherm contours. Axial velocity and temperature profiles at several heights and radius ratios are also presented to provide supplementary information. Heat transfer results are presented as the Nusselt number versus Rayleigh number and discussed to give details about heat transfer.

4.1 Fluid flow Structure

Representative streamline contours are presented in Fig. 3. The streamlines were assumed zero at all solid boundaries, and the figure consists of five diagrams, each showing the right-hand half of the vertical cross section for Ra = 10^5, A = 2, Pr = 0.7 and various radius ratios k = 1.2, 2, 4, 6 and 10. The negative sign for Ψ indicates clockwise circulation. The main feature of these flow fields is the circulation up along the heated side wall and down along the outer cold wall. The dimensionless stream function Ψ provides a direct index of the volumetric flow rate. The Ψ values for higher k were substantially lower than those for lower k, indicating decreased circulation. As the radius ratio k increases, the center of the circulation moves upward and towards the outer cylinder. This indicates that convection to the outer cylinder becomes stronger in the region closer to the top. With the decrease of the radius ratio the attraction for the flow towards the core of the cavity increases, and higher values of stream function exists also, carrying more convective heat from the hotter side to the colder one. The flow rate increases with the decrease of k, and the slope of the axis of the cells changes significantly from the vertical middle plane to the diagonal of the cavity. Therefore, the maximum velocities (horizontal and vertical components) drift from the vertical and horizontal middle planes to the corners (left bottom and right top corners).

An indication for the transport of energy by convection between the two boundary walls is the rate of flow inside the cavity, which can be expressed by the maximum value of the stream function which is defined as $\Psi_{max} = \max |\Psi(R,Z)|$. Figure 4 shows the behavior of this function with the increase of k for various Rayleigh numbers. The figure shows a significant decrease of Ψ_{max} with the increase of k indicating the decrease of the transport energy by convection part in the whole cavity. The figure shows a significant sharp decrease of Ψ_{max} with the increase of k indicating the decrease of the transport of energy by convection part in the whole cavity.

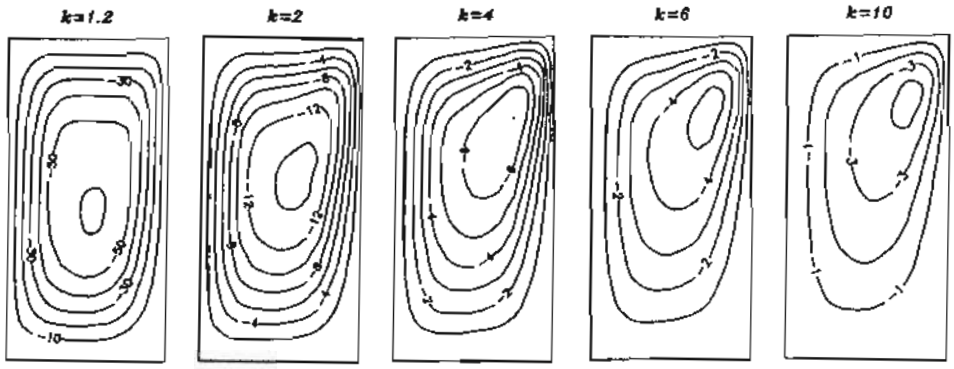

Fig. 3 Influence of the radius ratio k on the streamline distribution in the annulus for A=2, Pr=0.7 and Ra=10^5

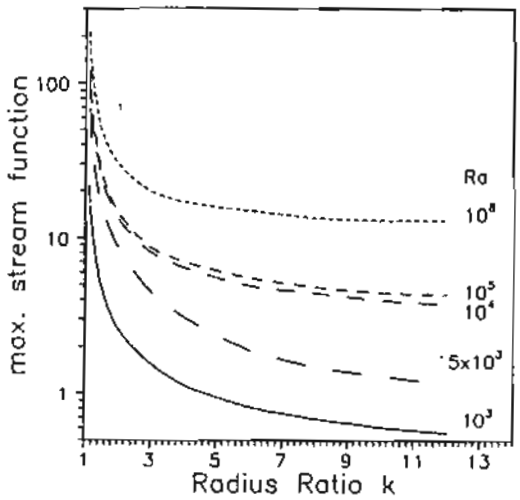

Fig. 4 Influence of the radius ratio k on the maximum stream function for A=2, Pr=0.7, and different Ra

4.2 Isotherms

Figure 5 presents dimensionless temperatures on the same format as the streamlines. In interpreting these diagrams, it should be remembered that the contour value at the outside wall is defined equal to zero.

With the increase of k, the isotherms in Fig. 5 moves in direction towards the top portion of the annulus and becomes closer to the lower part of the inner wall and the upper part of the outer wall. The isotherms will become increasingly crowded near the upper portion of the annulus. At high k, when the minimum temperature is close to the upper portion of the annulus and the higher point of the outer boundary wall, thermal boundary layers which are found in this region are indicated by the crowding together of the isotherms adjacent to the walls; vigorous heat transfer is to be expected in this region. In contrary the fluid in the lower portion of the annulus is becoming more nearly isothermal ($\theta \approx \theta_o = 0$).

4.3 Axial Velocity Profiles

Figure 6 shows several axial velocity distributions in an annulus with A=2, Pr = 0.7, Ra $=10^5$ for different radius ratios k =1.2, 2, 4, 6 and 10. Each diagram presents profiles at three different vertical positions: one at the center (designed by 1/2 H), one at one quarter height from the bottom (1/4 H) and one at one quarter height from the top (3/4 H) against R' where, R' is the nondimensional horizontal distance in the annulus $=(R-R_i)/(R_o-R_i)$. Figure 6 presents a boundary layer development at the side walls. which is indicated by the increased velocity gradient next to wall and the constant velocity profile in the middle. At the inner wall, the positive boundary flow is nearly the same with the change of the radius ratio. The maximum velocities occur in the center section for all radius ratios. At k=1.2 the velocity of both the top and bottom sections are nearly equal. With the increase of k the flow in the top section becomes faster and faster than that in the bottom section, until it equals the maximum velocity values of the center section at k=10. At the outer wall, the velocity of the flow decreases as the flow goes down. With the decrease of the radius ratio k the boundary layer becomes thinner and the maximum velocity increases.

4.4 Temperature Profiles

Figure 7 shows temperature profiles of five radius ratios at three different heights, the format and the nomenclature being the same as Fig. 6. The increasing slope at inner and outer wall and the increasing center core region show the development of the boundary layer at the side walls.

The heat and fluid flow structures elaborated in the foregoing section can be further inferred from the surface temperature of the constant heat flux inner wall. The effect of the radius ratio on the surface temperature on the heated inner wall is presented in Fig. 8 for A= 2, Pr = 0.7, Ra $=10^5$ and various radius ratios $1.2 \leq k \leq 10$

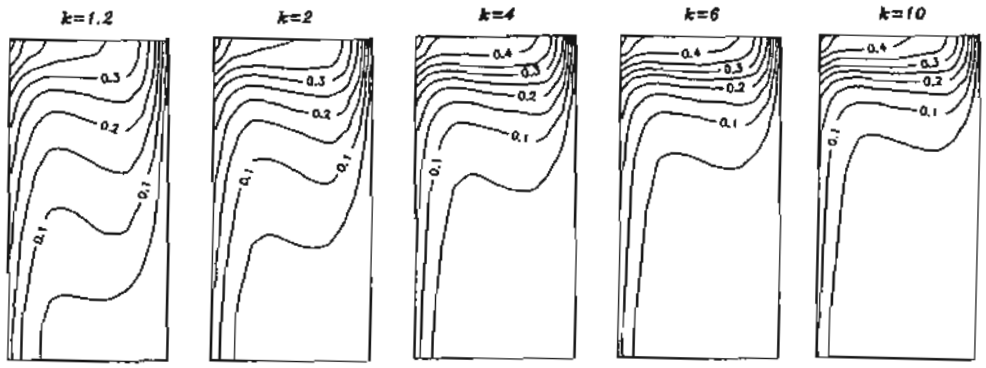

Fig. 5 Influence of the radius ratio k on the temperature contours for A=2, Pr=0.7 and Ra=10^5

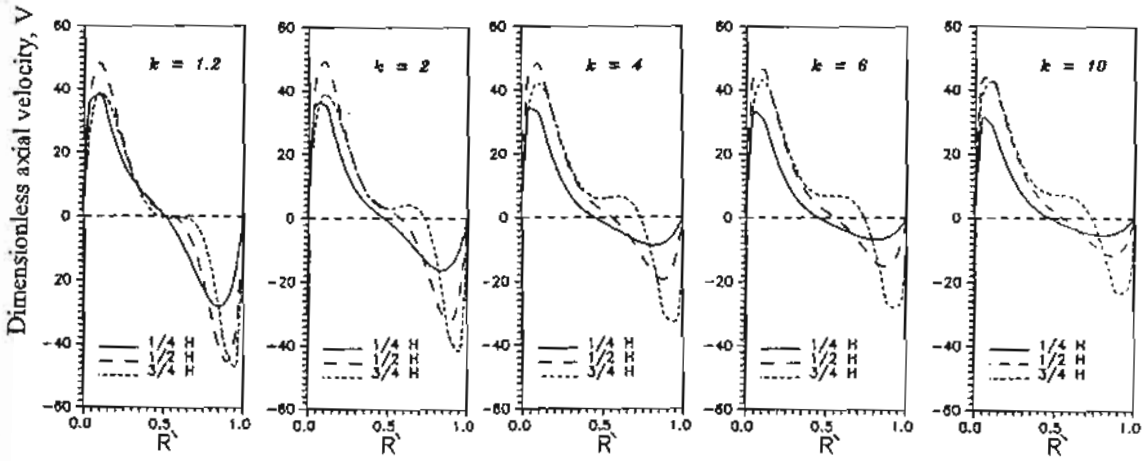

Fig. 6 Influence of the radius ratio k on the axial velocity distribution for A=2, Pr=0.7, Ra=10^5

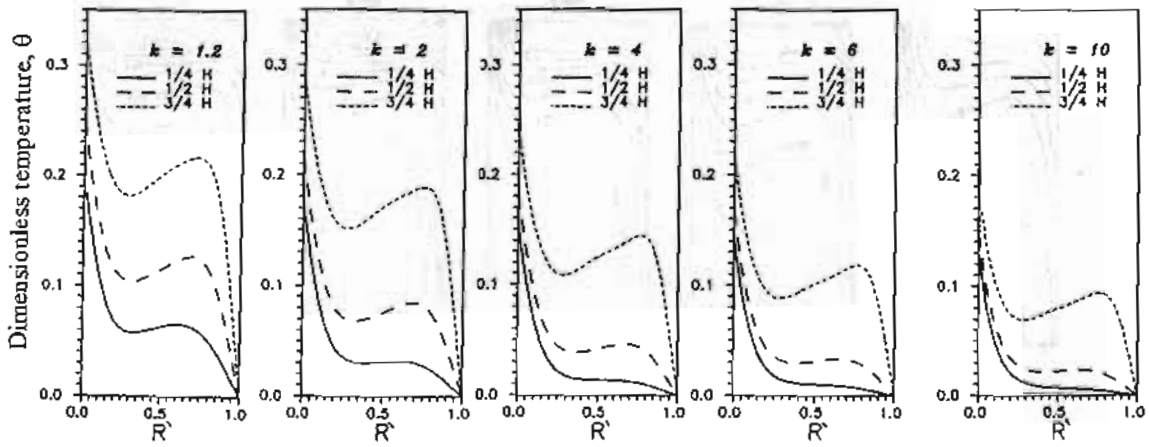

Fig. 7 Influence of the radius ratio k on the temperature profiles for A=2, Pr=0.7, Ra=10^5

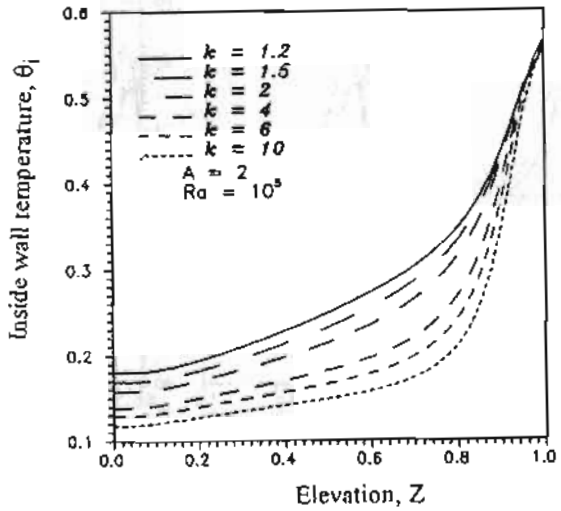

Fig. 8 effect of the radius ratio k on the inner surface temperature profiles for A=2, Pr=0.7, Ra=10^5

The surface temperature consistently increased from the bottom to the edge of the inner wall, which is indicative of clockwise circulation. While the maximum temperature at the edge of the inner wall is nearly constant for all radius ratios, the difference between the edge and bottom temperature increases with the increase of the radius ratio.

4.5 Heat Transfer

The average heat transfer coefficient at the inner wall is presented by means of an average Nusselt number defined as:

$$\bar{N}u = q\, D/[\, k(\, \bar{T}_i - T_o)] \qquad (10)$$

where $\bar{T}_i$ is the inside cylindet wall average temperature.

Figure 9 presents the relationship between the overall Nusselt number and the radius ratio for aspect ratio A=2 and different Rayleigh number ranging from 10^3 to 10^7. The increase of the radius ratio tends consistently to enhance the average heat transfer coefficient for all Rayleigh numbers considered in the figure. In order to reflect the convective contribution to the overall heat transfer for various radius ratio, the ratio of the averaged Nusselt number to that of pure conduction is presented in Fig. 10, where the average Nusselt number for pure conduction can be easily obtained as: $\bar{N}u_c = (k\text{-}1)/\log(k)$. Figure 10 clearly shows that by $Ra \le 10^3$ and for all values of k, $Nu/Nu_c = 1$ i.e. only pure conduction heat transfer exists. By $Ra > 10^3$ and with the increase of Ra, the contribution of the convective heat transfer mechanism increases. With the decreaase of the radius ratio k, the convective part of heat transfer increases signifying the increasing importance of convection heat transfer across the annulus.

In order to show the validity of the numerical simulation. an experimental test was done for the case of A= 41 and k=2 using the test rig shown in Fig. 2 The power input to the electric heater varied from 4 to 70 Watt. The radiative part of the electric heat input was calculated according to Thomas [12] and subtracted from the total heat input to get the convective and conductive part of the heat transferred. The measured convective and conductive average Nusselt number is calculated according to Eq. (10). The thermophysical properties of the air in both Nu and Ra terms are calculated at the mean temperature of the inner and outer annulus surfaces ($\bar{T}_{i+}\ \bar{T}_o)/2$. The measured average Nusselt number was compared with the corresponding simulated one. The comparison which is shown in Fig. 11 shows good agreement with maximum deviation of about 10 percent from those of the numerical results and validates the numerical model.

A comparison of the present results to those in the literature is difficult since no equivalent study exists except the work of Keyhani et. al. [6]. Keyhani et. al [6] modified a correlation for the average Nusselt number as follows:

$$\bar{N}u = 0.78\, A^{-0.052}\, k^{0.505}\, Ra^{0.072} \quad \text{for } 2.6\times10^3 \le Ra \le 1.8\times10^4 \quad \text{and}$$

$$\bar{N}u = 0.291\, A^{-0.238}\, k^{0.442}\, Ra^{0.244} \quad \text{for } 1.8\times10^4 \le Ra \le 4.21\times10^7 \qquad (11)$$

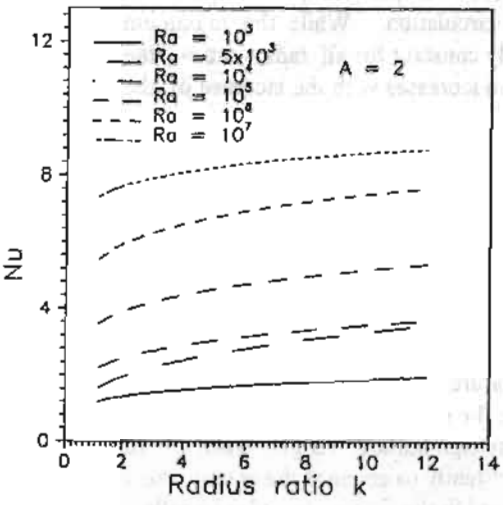

Fig. 9 Influence of the radius ratio k on the average Nusselt number for different Ra at A=2, Pr=0.7

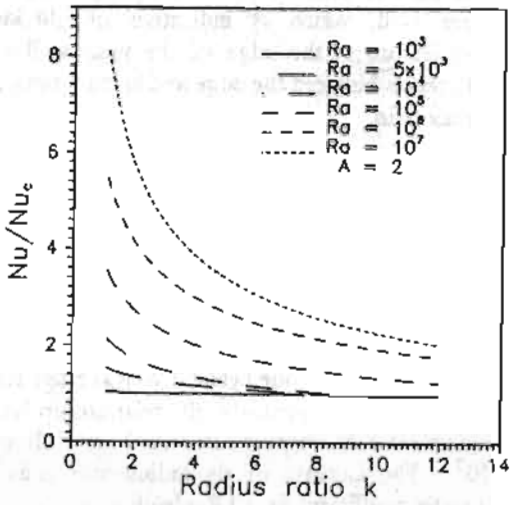

Fig. 10 Influence of the radius ratio k on the convective heat transfer contribution for different Ra at A=2, Pr=0.7

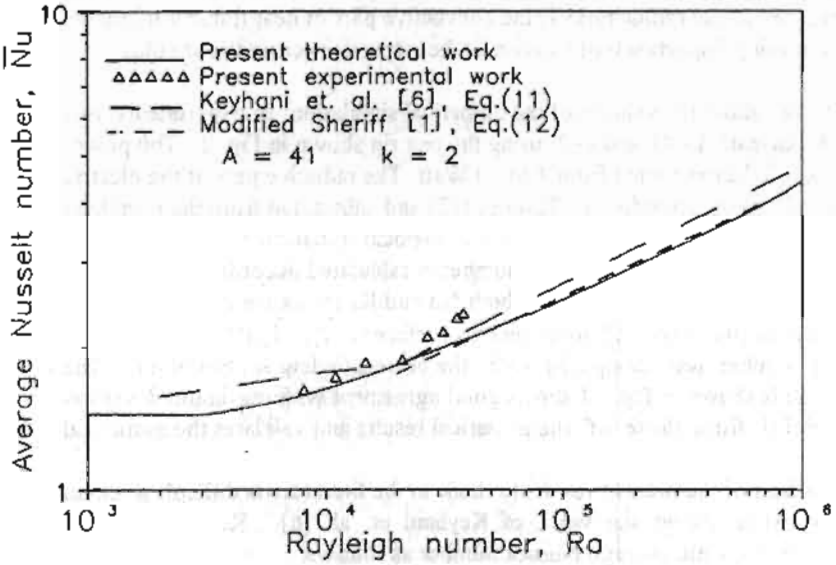

Fig. 11 Comparison between the numerical and the experimental average Nusselt number

It is also possible to modify the results of Sheriff [1] with the use of the results of Thomas and de Vahl Davis [4]. For the boundary layer regime, Thomas and de Vahl Davis [4] who studied the isothermal heated vertical annulus case, reported the Nusselt number dependence on the radius ratio and aspect ratio as $k^{0.442}$ and $A^{-0.25}$ respectively. Assuming that the dependence holds for the constant heat flux boundary condition at the inner wall, one can modify Sheriff's results which are represented by Eq. (1), to the following:

$$\bar{N}u = 0.3325\, A^{-0.25}\, k^{0.442}\, Ra^{0.231} \qquad (12)$$

A comparison of the present numerical and experimental results with those of Keyhani et. al. [6] Eq. (11) and Sheriff [1] Eq. (12) is presented in Fig. 11. The numerical results were nearly the same of those obtained from the Sheriff's modified equation and is about 5.5 to 10 percent lower than the results of Keyhani et . al. [6].

5. Conclusions

Numerical results are reported for the steady laminar natural convection of air in a vertical annulus with constant heat flux on the inner wall. The main object is to show the effect of radius ratio on the heat and fluid flow structures which are visualized by means of contour maps of streamlines and isotherms beside the axial velocity and temperature radial distribution. It is found that the radius ratio has a significant influence on the heat transfer process and the factors affecting it.

With the increase of radius ratio the maximum stream function decreases, the attraction for the flow changes from the core of the cavity upward towards the outer wall indicating stronger convection in this region, although it enhances the average heat transfer, the contribution of the convection part of heat transfer decreases signifying the increasing importance of conduction heat transfer across the annulus.

For all radius ratios the maximum velocities occur at the middle height. With the increase of radius ratio the flow in the top section becomes faster than that in the bottom section, the boundary layer becomes wider and the maximum velocity decreases.

With the increase of the radius ratio, the surface temperature of the constant heat flux inner wall increases from the bottom to the top, the difference between the top and bottom temperature increases, the isotherms moves in direction towards the top portion of the annulus and becomes closer to the lower part of the inner wall and the upper part of the outer wall and become increasingly crowded near the upper portion of the annulus and vigorous heat transfer is to be expected in this region.

6. Nomenclature

A	aspect ratio = H/D
D	gab width = $r_o - r_i$
H	annulus height, m
k	thermal conductivity,

k	radius ratio = r_o/r_i
Nu	Nusselt number
Nu_c	Nusselt number for pure conduction, = $(k - 1)/\log k$
P	pressure, Pa
Pr	Prandtle number
q	heat flux at the inner wall
r	radial coordinate
R	dimensionless radial coordinate
R'	dimensionless horizontal distance in the annulus =$(R-R_i)/(R_o - R_i)$
Ra	Rayleigh number
T	Temperature, K
u	velocity in the r direction, m/s
U	dimensionless velocity in the R direction
v	velocity in the z direction, m/s
V	dimensionless velocity in the Z direction
z	axial coordinate, m
Z	dimensionless axial coordinate
α	thermal diffusivity, m^2/s
β	volumetric coefficient of thermal expansion, 1/K
θ	dimensionless temperature
ψ	stream function
Ψ	dimensionless stream function
ζ	vorticity, 1/s
ω	dimensionless vorticity
ν	kinematic viscosity of the fluid, m^2/s
ρ	fluid density, kg/m^3

7. References

1. Sheriff, N., "Experimental Investigation of Natural Convection in Single and Multiple Vertical Annuli with High Pressure Carbon Dioxide," Proceedings, Third International Heat Transfer Conference, Chicago, Vol. 2, 1966, pp. 132-138.
2. Nagendra, H. R., Tirunarayanan, M. A., and Ramachandran, A., "Free Convection Heat Transfer in Vertical Annuli," Chemical Engineering Science, Vol. 5, 1970, pp. 605-610.
3. de Vahl Davis, G., and Thomas, R. W., "Natural Convection Between Concentric Vertical cylinder," High Speed Computing in Fluid Dynamics, Physics of Fluid, Supplement II, 1969, pp. 198-207.
4. Thomas, R, W., and de Vahl Davis, G., "Natural Convection in Annular and Rectangular Cavities. A Numerical Study," Proceedings, Fourth International Heat Transfer Conference, Paris, Vol. 4, Paper NC 2.4, Elsevier, Amsterdam 1970.
5. Schwab, T. H., and De Witt, K. J., "Numerical Investigation of Free Convection Between Two Vertical Coaxial Cylinders," AIChE J., Vol. 16, 1970, pp. 1005-1010.

6. Keyhani, M., Kulacki, F. A., and Christensen, R. N., "Free Convective In a Vertical Annulus with Constant Heat Flux on the Inner Wall," ASME J. of Heat Transfer, Vol. 105, 1983, pp. 454-459.
7. Bushan, R., Keyhani, M., Christensen, R. N., and Kulacki, F. A., "Correlation Equation for Free Convection in a Vertical Annulus with Constant Feat Flux on the Inner Wall," ASME J. of Heat Transfer, Vol. 105, 1983, pp. 910-912.
8. Prasad, V., and Kulacki, F. A., "Free Convection Heat Transfer in a Liquid-Filled Vertical Annulus," ASME Journal of Heat Transfer, Vol. 107, 1985, pp. 596-602.
9. Lin, D. S., and Nansteel, M. W., "Natural Convection in a Vertical Annulus Containing Water Near the Density Maximum," ASME J. of Heat Transfer, Vol. 109, 1987, pp. 899-905
10. Ho, C. J., and Lin, Y. H., "Natural Convection of Cold Water in a Vertical Annulus with Constant Heat Flux on the Inner Wall," ASME J. of Heat Transfer, Vol. 112, 1990, pp. 117-123
11. Patankar, S., "Numerical Heat Transfer and Fluid Flow" Mc Graw Hill, New York, 1980.
12. Thomas, L. C., "Heat Transfer" Prentice-Hall, Inc., Englewood Cliffs, New Jersey, USA, 1992, pp. 263.